

Ion Irradiation-Induced Easy-Cone Anisotropy in Double-MgO Free Layers for Perpendicular Magnetic Tunnel Junctions

B. M. S. Teixeira¹, A. A. Timopheev², N. F. F. Caçoilo¹, S. Auffret², R. C. Sousa², B. Dieny², E. Alves³, N. A. Sobolev^{1,4}

¹) Physics Department & i3N, University of Aveiro, 3810-193 Aveiro, Portugal

²) Université Grenoble Alpes, CEA, CNRS, Grenoble INP, INAC, SPINTEC, F-38000 Grenoble, France

³) IPFN, Instituto Superior Técnico, Universidade de Lisboa, 2695-066 Bobadela LRS, Portugal

⁴) National University of Science and Technology "MISIS", 119049 Moscow, Russia

Abstract

We have used the ferromagnetic resonance in the X-band (9.37 GHz) to investigate the effect of 400 keV Ar⁺ irradiation on the perpendicular magnetic anisotropy (PMA) and Gilbert damping parameter, α , of double-MgO free layers designed for application in perpendicular magnetic tunnel junctions. The samples comprised a MgO / Fe₇₂Co₈B₂₀ / X(0.2 nm) / Fe₇₂Co₈B₂₀ / MgO layer stack, where X stands for an ultrathin Ta or W spacer. Samples with two different total FeCoB layer thicknesses, $t_{\text{FCB}} = 3.0$ nm and $t_{\text{FCB}} = 2.6$ nm, were irradiated with ion fluences ranging from 10^{12} cm⁻² to 10^{16} cm⁻². The effective first-order PMA field, B_{K1} , decreased nearly linearly with the logarithm of the fluence for both FeCoB thicknesses and spacer elements. The decrease in B_{K1} , which is likely caused by an ion-induced intermixing at the FeCoB/MgO interfaces, resulted in a reorientation of the magnetization of the free layers with $t_{\text{FCB}} = 2.6$ nm, initially exhibiting a perpendicular easy-axis anisotropy. For intermediate fluences, 10^{13} cm⁻² and 10^{14} cm⁻², easy-cone states with different cone angles could be induced in the free layer with a W spacer. Importantly, no corresponding increase in the Gilbert damping was observed. This study shows that ion irradiation can be used to tune the easy-cone anisotropy in perpendicular magnetic tunnel junctions, which is interesting for spintronic applications such as spin-torque magnetic memories, oscillators and sensors.

Introduction

The interfacial perpendicular magnetic anisotropy (PMA) existing at the FeCoB/MgO interface is at the origin of the out-of-plane magnetized magnetic tunnel junctions (pMTJ) which serve as the basic storage elements of spin-transfer-torque magnetic random-access memory (STT-MRAM). These memories offer a higher storage density, higher thermal stability and lower power consumption than their in-plane counterparts¹.

For a sufficiently thin FeCoB film, the PMA overcomes the shape anisotropy, resulting in a perpendicular orientation of the magnetization. To increase the free(storage)-layer volume, V , and thus to improve the data retention, while keeping a strong PMA, two FeCoB/MgO interfaces may be used¹. To absorb the boron out of the FeCoB layers upon the post-deposition anneals required to recrystallize the MgO barrier and the FeCoB ferromagnetic (FM) electrodes, a thin metal (e.g., Ta, W) spacer is usually introduced in the middle of the FeCoB storage layer²⁻⁷. Besides improving the data retention, the double-MgO storage layer also exhibits a reduced Gilbert damping, α , as compared to thinner ones sandwiched between a single MgO barrier and a heavy-metal layer such as Ta or W. In the latter structures, a damping enhancement is often observed resulting from the spin-pumping effect. The suppression of spin pumping in the double-MgO free layers can result in a more than twofold decrease of the damping (and therefore of the critical current for switching, I_{c0}) accompanied by an almost doubling of PMA (and consequently, of the thermal stability factor, $\Delta = K_{\text{eff}}V/k_B T$, where K_{eff} is an effective PMA, k_B the Boltzmann constant and T the absolute temperature). The result is an overall improved switching efficiency, Δ/I_{c0} , which further increases as the pMTJ dimensions are reduced^{3,8}. Beside free layers for STT-MRAM, double-MgO free layers with a Ta spacer have also been proposed for the development of synthetic ferrimagnetic bilayers⁹ as well as remnant spin injectors onto GaAs-based light emitting diodes¹⁰.

One issue associated with pMTJ stacks is the stochasticity of the STT switching, as a misalignment between the fixed- and free-layer magnetization is necessary for a transfer of angular momentum by a spin-polarized current to occur. Such a misalignment is introduced by thermal fluctuations, but these cause a broad distribution of the switching times due to their random nature. As shown by analytical calculations¹¹ and macrospin simulations¹², setting the free layer in a magnetic easy-cone state, with the cone angle providing the misalignment, would greatly improve the switching characteristics of the pMTJ. Such an easy-cone state is described by phenomenologically including a second-order term, K_2 , in the PMA energy density of a thin film, in addition to the first-order term, K_1 , i.e., $U_{\text{PMA}} = -K_1 \cos^2\theta - K_2 \cos^4\theta$, with θ being the angle between the magnetization and the normal to the film plane. An easy-cone equilibrium state emerges when $K_1 > 0$, $K_2 < 0$ and $-K_2/K_1 > 0.5$. Beside certain alloys (e.g., NdCo₅ (Ref.¹³) and Mn₂RhSn (Ref.¹⁰)), multi-layers containing the FeCoB/MgO interface can also exhibit easy-cone anisotropy, when the FeCoB thickness is properly adjusted to be close to the reorientation from out-of-plane to in-plane anisotropy¹⁴⁻¹⁹.

It has been analytically shown that a negative K_2 can arise from spatial fluctuations of K_1 (Ref.²⁰). In our previous study on granular MgO/FeCoB/Ta (Ref.¹⁷) the micromagnetic origin of K_2 was demonstrated and it was shown that its magnitude was determined by the ratio between the thickness-dependent magnetic inhomogeneities, such as spatial fluctuations of K_1 , and the intergrain exchange coupling. Another approach to explain the origin of K_2 , proposed by J. Sun²¹, considers the simultaneous presence of two effects: weakening of the exchange near the MgO/FM interface and a strong interface-concentrated PMA efficiently acting only on the very first atomic layers of the magnetic film. In this case, the resulting ‘exchange-spring’-like effect can also be at the origin of a negative K_2 .

One should notice that the easy-cone anisotropy can be useful not only for STT-MRAM but also for other spintronic applications such as spin-torque oscillators²² and magnetic sensors^{11,19}. However, reproducibly controlling the easy-cone anisotropy in FeCoB/MgO systems may be technologically challenging, as this state is only found within a narrow range of layer thicknesses. It would thus be desirable to find a post-deposition process for reorienting the magnetization direction via the control of the interfacial PMA. In that regard, high-energy particle irradiation appears as a simple and reproducible tool to physically modify the interfaces and thus control interfacial magnetic phenomena. A review of the work published in this field until 2004 is given in Ref.²³. Light ion (He^+) irradiation has been used to reduce the PMA in Pt/Co multilayers by promoting local intermixing at the interfaces²⁴ and thus to manipulate the magnetization direction of such systems, from out-of-plane to in-plane and also to oblique orientations²⁵. Heavier ions such as Ar^+ were used to modify the properties of Pt/Co films as well²⁶. More recently, He^+ irradiation was used to manipulate the direction of the exchange-bias field in MTJ stacks²⁷, to reduce the annealing temperature for crystallizing CoFeB in MgO-based MTJs²⁸, and to control the domain wall velocity²⁹. Here, we explore the possibility of inducing an easy-cone anisotropy in the technologically relevant MgO/FeCoB/MgO free layers, with and without inclusion of Ta or W spacers, by 400 keV Ar^+ irradiation.

Experimental details

Free layers composed of Ta(3) / Ru(2) / W(3) / Ta(1) / FeCoB(0.3) / MgO(1.3) / FeCoB(1.4) / X(0.2) / FeCoB(t) / MgO(1.1) / W(2) / Pt(3), where X stands for a Ta or W spacer, and FeCoB is a $\text{Fe}_{72}\text{Co}_8\text{B}_{20}$ alloy, were deposited by magnetron sputtering onto a thermally oxidized 4-inch Si wafer and annealed at 300°C for 2 min. The numbers in parentheses are nominal thicknesses in nanometers. The total thickness of the FeCoB free layer ($t_{\text{FCB}} = 1.4 + t$ nm) was varied by growing the topmost FeCoB layer as a wedge ($0.4 < t < 1.6$ nm). Free layers with equal thickness but without spacer were also prepared. Details regarding the sample preparation can be found in Ref.³⁰ for similarly prepared structures.

Samples with an area of 4×4 mm² were cut from the wafer ensuring a negligible (± 0.18 Å) nominal thickness gradient. Two thicknesses of the FeCoB layer were selected for two irradiation runs: $t_{\text{FCB}} = 3.0$ nm and $t_{\text{FCB}} = 2.6$ nm. The irradiation with 400 keV Ar^+ ions was performed at five

different fluences, Φ , ranging from 10^{12} cm⁻² to 10^{16} cm⁻². The irradiation conditions guarantee that elastic and inelastic interactions occur within the multilayers, with expected intermixing of elements across the interfaces (changes in the element concentration profiles smaller than 7×10^{-14} in units of $\% \Phi^{-1}$), whereas the Ar⁺ ions are deposited inside the Si substrate (not shown), as simulated by the TRIM (Transport of Ions in Matter) package included in the SRIM software³¹.

The magnetic properties of the free layers were investigated using angle-dependent ferromagnetic resonance (FMR) measurements performed at room temperature at a microwave frequency of 9.37 GHz in an EPR spectrometer. To account for small variability of magnetic properties of the free layers cut from the same wafer, the FMR spectra were acquired for all samples before and after irradiation. From the out-of-plane angular dependence of the resonance field, B_{res} (see, e.g., [figure 3](#)), we estimated the first- and second-order anisotropy contributions, starting from the description of the magnetic free-energy density:

$$\frac{U}{M_S} = -B \cos(\theta_B - \theta_M) - \frac{1}{2} B_{K1} \cos^2 \theta_M - \frac{1}{4} B_{K2} \cos^4 \theta_M, \quad (1)$$

where $B_{K1} = (2k_{s1}/(t_{\text{FCB}}M_S)) - 4\pi M_S$ is the effective first-order anisotropy field resulting from the competing contributions of the interfacial PMA ($2k_{s1}/t_{\text{FCB}}$) and the thin-film shape anisotropy ($4\pi M_S^2$); $B_{K2} = 4K_2/M_S$ is the effective second-order anisotropy field; k_{s1} is the first-order interfacial PMA constant; K_2 the second-order volume PMA constant; M_S the saturation magnetization, and θ_M (θ_B) the angle between the magnetization (external field) and the film normal. For details of the general development of the model to extract the FMR modes, $\omega(B)$, see, e.g., Refs. [13,32](#).

Results

The 3.0-nm-thick FeCoB layers originally exhibited an easy-plane anisotropy, while the 2.6-nm-thick layers with a Ta or W spacer were initially in the easy-axis regime, with the magnetization oriented along the film normal. [Table I](#) summarizes the mean values and standard deviations of the anisotropy fields extracted before irradiation, $B_{K1,2}^0$, for the different spacer and film thickness configurations. After irradiation, the anisotropy fields, B_{Ki}^F , were extracted for each ion fluence, and the variations of B_{Ki} were calculated as $\delta(B_{Ki}) = B_{Ki}^F - B_{Ki}^0$, $i = 1, 2$ ([figure 1](#)).

After irradiation, the FMR line shifted toward higher (lower) fields for out-of-plane (in-plane) applied magnetic field. Interestingly, as the line shifted, additional weaker resonances became evident (not shown). Up to this moment we have not developed a physical understanding of those additional lines and limited the following analysis to the main FMR line (i.e. the line evident both before and after irradiation).

Table I: Mean first- and second-order anisotropy fields extracted before irradiation.

Free layer	B_{K1}^0 (kG)	B_{K2}^0 (kG)
MgO/ FeCoB(3.0)/ MgO	-4.098 ± 0.046	-0.279 ± 0.016
MgO / FeCoB(1.4) / W(0.2) / FeCoB(1.6) / MgO	-0.402 ± 0.036	-0.689 ± 0.004
MgO / FeCoB(1.4) / Ta(0.2) / FeCoB(1.6) / MgO	-0.865 ± 0.058	-0.492 ± 0.003
MgO / FeCoB(1.4) / W(0.2) / FeCoB(1.2) / MgO	0.939 ± 0.125	-0.424 ± 0.016
MgO / FeCoB(1.4) / Ta(0.2) / FeCoB(1.2) / MgO	0.838 ± 0.040	-0.402 ± 0.004

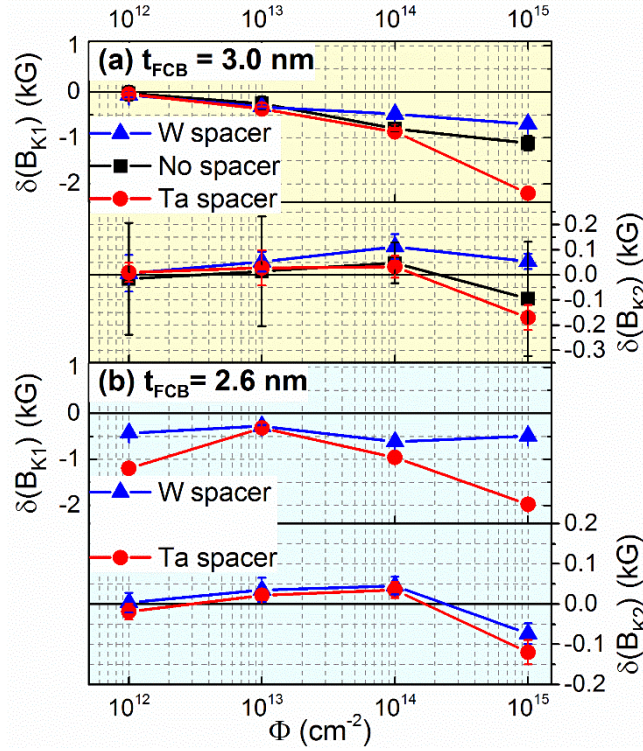


Figure 1: Absolute variation of the first- and second-order anisotropy fields with ion fluence ($\delta(B_{Ki}) = B_{Ki}^F - B_{Ki}^0$) for (a) 3.0-nm-thick and (b) 2.6-nm-thick FeCoB films with a W spacer (triangles), Ta spacer (dots) or no spacer (squares). **Table 1** provides the reference values before irradiation, B_{Ki}^0 , for each of the layers.

The top panels of **figures 1a)** and **1b)** show the nearly linear decrease of B_{K1} with the logarithm of the ion fluence for $t_{FCB} = 3.0$ nm and $t_{FCB} = 2.6$ nm, respectively. While a fluence of 10^{12} cm^{-2} produces almost no change in anisotropy for the 3.0-nm-thick sample, at 10^{15} cm^{-2} the B_{K1} value decreases significantly in the free layers with the W spacer, no-spacer and Ta spacer by about -0.7 kG, -1.1 kG and -2.2 kG, respectively. In the 2.6 nm-thick free layer, a decrease of B_{K1} also occurs (the 10^{12} cm^{-2} point is treated as an outlier, and the value for 10^{15} cm^{-2} and the W spacer may be explained by an increased inhomogeneity of the initial sample inherent to these thinner layers). Both irradiation runs showed a higher decrease in B_{K1} when the Ta spacer was

used instead of the W one. A slight decrease of $|B_{K2}|$ with the ion fluence increasing up to 10^{14} cm^{-2} was also observed (bottom panels of figures 1a) and 1b)). At 10^{16} cm^{-2} the FMR line disappeared in all cases, probably due to a strong sample intermixing inducing a ferromagnetic-paramagnetic transition. Both the nearly unchanged B_{K1} for $\Phi = 10^{12}$ cm^{-2} and the lack of FMR at $\Phi = 10^{16}$ cm^{-2} are consistent with the order of magnitude found in the TRIM simulations for the maximum profile concentration changes (around $7 \times 10^{-14} \% \Phi^{-1}$).

Looking at the definition of B_{K1} , its decrease can be explained either by an increase of M_S or by a decrease of k_{s1} . Reports on Co thin films (0.5 nm) have shown M_S to decrease upon a 10^{16} cm^{-2} He^+ irradiation at 30 keV (Ref. 25). In Ref. 33, the authors reported an unchanged M_S of Co/Pd/Co/Ni multilayers irradiated with up to 10^{15} He^+/cm^2 at 20 keV. Assuming M_S does not increase with the ion irradiation in our case, which is reasonable when accounting for the loss of the magnetic ordering observed for $\Phi = 10^{16}$ cm^{-2} , the reduction of B_{K1} may be ascribed to a drop of k_{s1} . Like in Ref. 25, this is consistent with an elemental mixing at the FeCo/MgO interface, in our case modifying interfacial Fe(Co)-O electronic hybridization at the origin of the PMA and thus resulting in a reduction of k_{s1} . Furthermore, heavier ions, such as Ar^+ , are more efficient in ballistic- and defect-enhanced diffusion intermixing at the interfaces than He^+ , due to a higher energy deposition in elastic collisions. Indeed, for equal energies, lower fluences of Ar^+ than of He^+ have been shown to reduce the coercivity by the same amount 26. Irradiation-induced migration of B, W or Ta to the FeCoB/MgO interface or alloying of these elements with Fe may also lead to a local decrease of k_{s1} , as well as to a reduction of M_S .

Several investigations 24-26 reported similar irradiation-induced modulations of B_{K1} in Co/Pt multilayers with interfacial PMA, attributing their origin to interfacial mixing. Here we have shown that the PMA in the MgO/FeCoB/MgO system decreases with increasing Ar^+ ion fluence. The anisotropy modulation resulted in a reorientation of the magnetization direction: while the 3.0-nm-thick free layers were driven deeper into the easy-plane regime, spin reorientations were effectively induced in the free layers with $t_{\text{FCB}} = 2.6$ nm, as highlighted in figure 2.

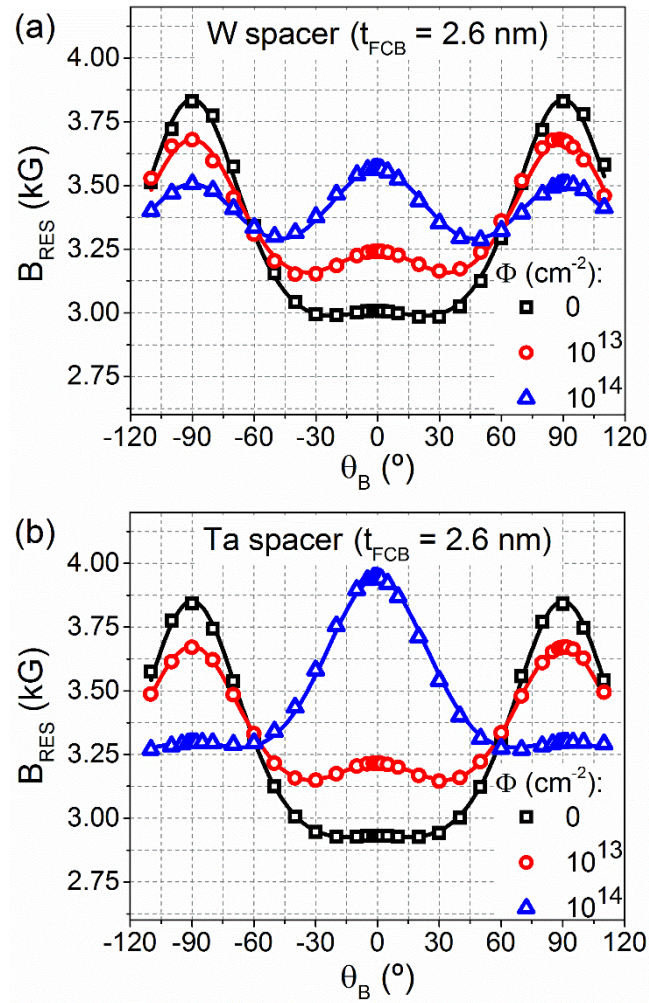


Figure 2: Out-of-plane angular dependences of the resonance field, for $t_{FCB} = 2.6$ nm with a W (a) or Ta (b) spacer for different ion fluences: 0 cm^{-2} (squares), 10^{13} cm^{-2} (dots) and 10^{14} cm^{-2} (triangles). The solid lines are fits to the data.

The free layer with a W spacer initially exhibits a uniaxial perpendicular magnetic anisotropy. After an Ar^+ irradiation with 10^{13} cm^{-2} and 10^{14} cm^{-2} , the magnetization is driven into the easy-cone state with the cone angle increasing to 30° and 45° , respectively. In the free layer with a Ta spacer, the stronger decrease of B_{K1} leads to a complete reorientation of the magnetization from easy axis (before irradiation) to easy cone at 10^{13} cm^{-2} and then to easy plane at 10^{14} cm^{-2} .

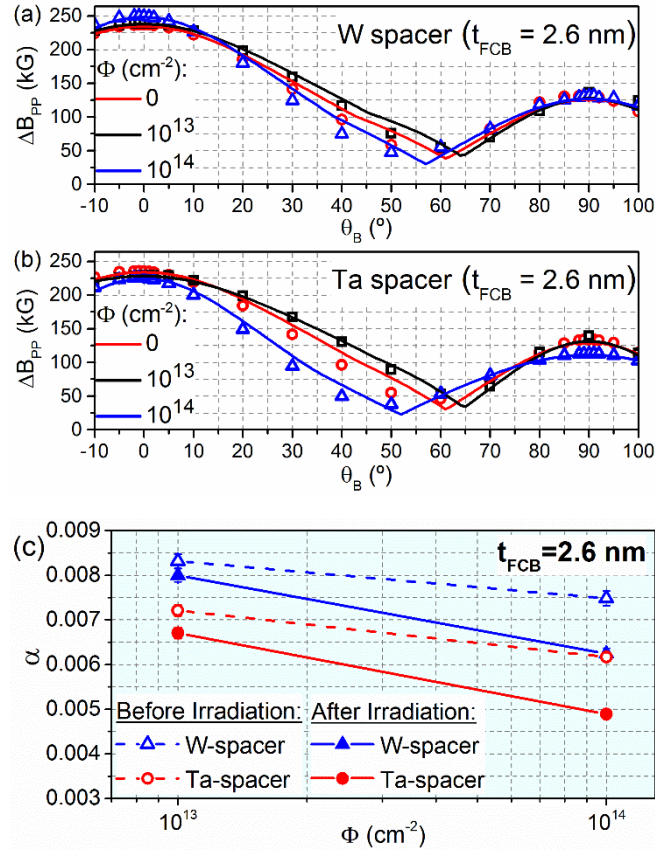


Figure 3: (a-b) Out-of-plane angular dependences of the peak-to-peak linewidth, for $t_{\text{FCB}} = 2.6 \text{ nm}$ with a W (a) or Ta (b) spacer for different irradiation fluences: 0 cm^{-2} (squares), 10^{13} cm^{-2} (dots) and 10^{14} cm^{-2} (triangles). The solid lines are fits to the data. (c) Gilbert damping parameter extracted before (open symbols and dashed lines) and after (solid symbols and lines) irradiation.

The effect of the irradiation on the peak-to-peak linewidth, ΔB_{PP} , was also assessed for those free layers whose magnetization direction was reoriented (figures 3a) and 3b). We modelled the $\Delta B_{PP}(\theta_M)$ dependence using two contributions to the linewidth: the intrinsic one, proportional to the Gilbert damping, α , and the inhomogeneous one caused by fluctuations of the anisotropy fields, $\Delta(B_{K_i})$. Fluctuations of the anisotropy direction, $\Delta\theta_B$, were found to be negligible in our layers. Following the method of Ref. 34, ΔB_{PP} is written as a first-order Taylor series expansion of $\Delta B_{PP}^{K_i}$ and ΔB_{PP}^α versus the broadening contributions, $\Delta(B_{K_i})$ and $\Delta\omega = \alpha\gamma(\partial^2 U / \partial\theta_M^2)$, as:

$$\Delta B_{PP} = \frac{1}{\sqrt{3}} \left(\Delta(B_{K_i}) \left| \frac{\partial B_{RES}}{\partial B_{K_i}} \right| + \alpha\gamma \frac{\partial^2 U}{\partial\theta_M^2} \left| \frac{\partial B_{RES}}{\partial\omega} \right| \right) \quad (2)$$

where γ and ω are the gyromagnetic ratio and the magnetization precession frequency, respectively.

We found the linewidth to be dominated by the inhomogeneous broadening caused by spatial fluctuations of B_{K_1} : the lines are broader for $\theta_B = 0^\circ$ than for $\theta_B = 90^\circ$, and at an intermediate angle the inhomogeneous contribution is cancelled out (i.e. the $B_{RES}(\theta)$ dependencies calculated for a fluctuating B_{K_1} coincide in one angular point, where $\partial B_{RES} / \partial B_{K_1} = 0$), resulting in narrower lines.

The intrinsic broadening, on the other hand, has a different angular dependence, with equal minima found at $\theta_B = 0^\circ$ and $\theta_B = 90^\circ$ and can therefore be distinguished from the inhomogeneous one during the fitting. From the fittings of figures 3a) and 3b), we made the estimation of α reported in figure 3c).

Compared to the values extracted before irradiation (open symbols and dashed lines in figure 3), α appears to have decreased for the free layers irradiated with fluences of 10^{13} cm^{-2} and 10^{14} cm^{-2} . These α values, ranging from approximately 0.008 to 0.004, are quite reasonable considering the thickness of the FeCoB films in our double-MgO structures. Similar values were obtained in Refs.^{35,36} for Ta/CoFeB/MgO structures with similar thicknesses of the CoFeB layer.

Summarizing, we have shown that Ar^+ irradiation can induce an easy-cone state in MgO/FeCoB/MgO free layers with metallic spacers, without increasing the Gilbert damping, which is a prerequisite to keep a low STT-switching current. In principle, a fine tune of the irradiation conditions such as ion mass, energy and fluence may enable a more refined control of the easy-cone angle with a minimal decrease of the PMA. Nevertheless, the development of an irradiation technology of pMTJ will require a full understanding of the extent of the sample damage caused by the irradiation, especially its influence on the tunnel magnetoresistance. From a fundamental viewpoint, ion irradiation may be useful to study interface-induced magnetic phenomena, namely, the effect of the distribution of PMA and of the exchange coupling on the emergence of the second-order anisotropy.

Conclusions

We irradiated MgO / FeCoB(t_{FCB}) / MgO free layers, with and without a 0.2-nm-thick W or Ta spacer, and $t_{\text{FCB}} = 3.0 \text{ nm}$ or $t_{\text{FCB}} = 2.6 \text{ nm}$, with 400 keV Ar^+ ions at fluences ranging from 10^{12} cm^{-2} to 10^{16} cm^{-2} . The effective first-order PMA field, B_{K1} , decreased linearly with the logarithm of the fluence, from 10^{12} cm^{-2} to 10^{15} cm^{-2} . We suggest this decrease in B_{K1} to be a consequence of ion-induced intermixing at the FeCoB/MgO interface.

We have shown that the decrease in PMA caused by the ion irradiation induces spin reorientations in these free layers. While the 3.0-nm-layer remains in its original easy-plane regime, we effectively produce easy-cone anisotropy, with different cone angles, in the thinner layer (2.6 nm) with a W spacer and obtain a complete spin reorientation from easy axis to easy cone and then to easy plane in the free layer with a Ta spacer. Importantly, the irradiation, at fluences for which these transitions occur, did not increase the Gilbert damping parameter, which is vital, from an application viewpoint, to keep a low current density for STT-switching.

Acknowledgments

B.M.S.T. and N.A.S. acknowledge financial support of the FCT of Portugal through Project No. I3N/FSCOSD (Reference No. FCT UID/CTM/50025/2013) and through the bursary

PD/BD/113944/2015, as well as from the European project H2020-MSCA-RISE-2017-778308 - SPINMULTIFILM. This study was also partially funded by ERC Adv. Grant MAGICAL No. 669204. A.A.T. acknowledges partial support of the Samsung Global MRAM Innovation Program, CEA-EUROTALENTS fellowship.

References

- ¹ B. Dieny and M. Chshiev, *Rev. Mod. Phys.* **89**, 25008 (2017).
- ² H. Sato, M. Yamanouchi, S. Ikeda, S. Fukami, F. Matsukura, and H. Ohno, *IEEE Trans. Magn.* **49**, 4437 (2013).
- ³ H. Sato, E.C.I. Enobio, M. Yamanouchi, S. Ikeda, S. Fukami, S. Kanai, F. Matsukura, and H. Ohno, *Appl. Phys. Lett.* **105**, 62403 (2014).
- ⁴ E.C.I. Enobio, H. Sato, S. Fukami, F. Matsukura, and H. Ohno, *IEEE Magn. Lett.* **6**, 5700303 (2015).
- ⁵ J.-H. Kim, J.-B. Lee, G.-G. An, S.-M. Yang, W.-S. Chung, H.-S. Park, and J.-P. Hong, *Sci. Rep.* **5**, 16903 (2015).
- ⁶ H. Almasi, M. Xu, Y. Xu, T. Newhouse-Illige, and W.G. Wang, *Appl. Phys. Lett.* **109**, 32401 (2016).
- ⁷ S. Couet, T. Devolder, J. Swerts, S. Mertens, T. Lin, E. Liu, S. Van Elshocht, and G. Sankar Kar, *Appl. Phys. Lett.* **111**, 152406 (2017).
- ⁸ D. Apalkov, B. Dieny, and J.M. Slaughter, *Proc. IEEE* **104**, 685 (2016).
- ⁹ P. Pirro, A. Hamadeh, M. Lavanant-Jambert, T. Meyer, B. Tao, E. Rosario, Y. Lu, M. Hehn, S. Mangin, and S. Petit Watelot, *J. Magn. Magn. Mater.* **432**, 260 (2017).
- ¹⁰ B.S. Tao, P. Barate, J. Frougier, P. Renucci, B. Xu, A. Djeflal, H. Jaffrès, J.M. George, X. Marie, S. Petit-Watelot, S. Mangin, X.F. Han, Z.G. Wang, and Y. Lu, *Appl. Phys. Lett.* **108**, 152404 (2016).
- ¹¹ H. Arai, R. Matsumoto, S. Yuasa, and H. Imamura, *Appl. Phys. Express* **8**, 83005 (2015).
- ¹² N. Strelkov, A. Timopheev, R.C. Sousa, M. Chshiev, L.D. Buda-Prejbeanu, and B. Dieny, *Phys. Rev. B* **95**, 184409 (2017).
- ¹³ B.M.S. Teixeira, A.A. Timopheev, R. Schmidt, M.R. Soares, M. Seifert, V. Neu, and N.A. Sobolev, *J. Phys. D: Appl. Phys.* **49**, 315002 (2016).
- ¹⁴ A.A. Timopheev, R. Sousa, M. Chshiev, T. Nguyen, and B. Dieny, *Sci. Rep.* **6**, 26877 (2016).
- ¹⁵ J.M. Shaw, H.T. Nembach, M. Weiler, T.J. Silva, M. Schoen, J.Z. Sun, D.C. Worledge, T.J. Watson, and Y. Heights, *IEEE Trans. Magn.* **6**, 3500404 (2015).
- ¹⁶ Y. Fu, I. Barsukov, J. Li, A.M. Gonçalves, C.C. Kuo, M. Farle, and I.N. Krivorotov, *Appl. Phys. Lett.* **108**, 142403 (2016).
- ¹⁷ A.A. Timopheev, B.M.S. Teixeira, R.C. Sousa, S. Aufret, T.N. Nguyen, L.D. Buda-Prejbeanu, M. Chshiev, N.A. Sobolev, and B. Dieny, *Phys. Rev. B* **96**, 14412 (2017).
- ¹⁸ K.-W. Park, J.-Y. Park, S.C. Baek, D.-H. Kim, S.-M. Seo, S.-W. Chung, and B.-G. Park, *Appl. Phys. Lett.* **109**, 12405 (2016).

- ¹⁹ Y. Aleksandrov, C. Fowley, E. Kowalska, V. Sluka, O. Yildirim, J. Lindner, B. Ocker, J. Fassbender, and A.M. Deac, *AIP Adv.* **6**, 65321 (2016).
- ²⁰ B. Dieny and A. V Vedyayev, *Europhys. Lett.* **25**, 723 (1994).
- ²¹ J.Z. Sun, *Phys. Rev. B* **91**, 174429 (2015).
- ²² R. Matsumoto, H. Arai, S. Yuasa, and H. Imamura, *Phys. Rev. B* **92**, 140409(R) (2015).
- ²³ J. Fassbender, D. Ravelosona, and Y. Samson, *J. Phys. D: Appl. Phys.* **37**, R179 (2004).
- ²⁴ C. Chappert, H. Bernas, J. Ferré, V. Kottler, J.-P. Jamet, Y. Chen, E. Cambriil, T. Devolder, F. Rousseaux, V. Mathet, and H. Launois, *Science* **280**, 1919 (1998).
- ²⁵ J. Ferré, T. Devolder, H. Bernas, J.-P. Jamet, V. Repain, M. Bauer, N. Vernier, and C. Chappert, *J. Phys. D: Applied Phys.* **36**, 3103 (2003).
- ²⁶ C.T. Rettner, S. Anders, J.E.E. Baglin, T. Thomson, and B.D. Terris, *Appl. Phys. Lett.* **80**, 279 (2002).
- ²⁷ V. Höink, M.D. Sacher, J. Schmalhorst, G. Reiss, D. Engel, D. Junk, and A. Ehresmann, *Appl. Phys. Lett.* **86**, 152102 (2005).
- ²⁸ T. Devolder, I. Barisic, S. Eimer, K. Garcia, J.P. Adam, B. Ockert, and D. Ravelosona, *J. Appl. Phys.* **113**, 203912 (2013).
- ²⁹ L. Herrera Diez, F. García-Sánchez, J.-P. Adam, T. Devolder, S. Eimer, M.S. El Hadri, A. Lamperti, R. Mantovan, B. Ocker, and D. Ravelosona, *Appl. Phys. Lett.* **107**, 32401 (2015).
- ³⁰ L. Cuchet, R.C. Sousa, L. Vila, S. Auffret, B. Rodmacq, and B. Dieny, *IEEE Trans. Magn.* **50**, 4401404 (2014).
- ³¹ J.F. Ziegler, M.D. Ziegler, and J.P. Biersack, *Nucl. Instr. Methods Phys. Res. B* **268**, 1818 (2010).
- ³² S.M. Rezende, C. Chesman, M. A. Lucena, A. Azevedo, F.M. de Aguiar, and S.S.P. Parkin, *J. Appl. Phys.* **84**, 958 (1998).
- ³³ J.M.L. Beaujour, A.D. Kent, D. Ravelosona, I. Tudosa, and E.E. Fullerton, *J. Appl. Phys.* **109**, 33917 (2011).
- ³⁴ S. Mizukami, Y. Ando, and T. Miyazaki, *Jpn. J. Appl. Phys.* **40**, 580 (2001).
- ³⁵ X. Liu, W. Zhang, M.J. Carter, and G. Xiao, *J. Appl. Phys.* **110**, 33910 (2011).
- ³⁶ S. Iihama, S. Mizukami, H. Naganuma, M. Oogane, Y. Ando, and T. Miyazaki, *Phys. Rev. B* **89**, 174416 (2014).